

Phosgene formation from the decomposition of 1,1-C₂H₂Cl₂ contained gas in an RF plasma reactor

Wen-Jhy Lee^{a,*}, Chuh-Yung Chen^b, Wen-Chang Lin^a,
Ying-Tang Wang^a, Ching-Ju Chin^a

^aDepartment of Environmental Engineering, National Cheng Kung University, Tainan 70101, Taiwan

^bDepartment of Chemical Engineering, National Cheng Kung University, Tainan 70101, Taiwan

Received 15 March 1995; accepted 20 August 1995

Abstract

In this study, a radio-frequency (RF) plasma system was used to decompose the 1,1-dichloroethylene (DCE) contained gas. The reactants and final products were analyzed by using an FTIR (Fourier Transform Infrared Spectroscopy). The effect of plasma operational-parameters for DCE decomposition was evaluated. In addition, the possible reaction pathways for DCE decomposition and phosgene (COCl₂) formation were built up and discussed. Both DCE decomposition efficiency and the fraction of total carbon mass converted into CO₂ and CO were decreased by the increasing DCE feeding concentration. The DCE decomposition efficiency at varied equivalence ratios, ϕ (stoichiometric O₂/actual O₂), was controlled by both oxidation and energy transfer efficiency. At lower equivalence ratios having an excess of oxygen, a larger amount of COCl₂ was formed due to a higher oxygen-feeding concentration. Higher input power wattage can increase both the DCE decomposition efficiency and the fraction of total-carbon mass converted into CO₂ and CO, resulting in the reduction of the COCl₂ effluent concentration. However, more soot was found in the plasma reactor when the input power wattage was higher than 60 W. Because high concentrations of C₂Cl₄, CHCl₃ and CCl₄ were detected and because copper inner-electrode might act as catalyst, the most possible pathways for the COCl₂ formation were C₂Cl₄ + OH, C₂Cl₃ + O₂, CHCl₃ + O, CHCl₂ + O, CCl₃ + O and CO + Cl₂.

Keywords: Phosgene; Reaction; Dichloroethylene; Chlorinated hydrocarbons; Plasma

1. Introduction

Phosgene (COCl₂) is a colorless, volatile, and highly toxic gas. It was originally manufactured as an agent for chemical warfare but is now used commercially as a

* Corresponding author.

basic monomer or an intermediate in the synthesis of a wide variety of industrial agents. For example, phosgene is an intermediate in the production of toluene diisocyanate, isocyanates, and polycarbonate resins. These three products account for 55%, 30%, and 7% respectively, of the total use of phosgene as an intermediate in chemical manufacturing [1]. Phosgene can be produced by mixing carbon monoxide and chlorine when a catalyst exists. Thermal and photochemical decomposition of chlorinated hydrocarbons also forms phosgene [2].

Chlorinated hydrocarbons (CHCs) are important compounds for industrial use. CHCs are associated with the formation of chlorinated aromatics, dibenzodioxins, dibenzofurans, and other highly toxic compounds like phosgene [3–6]. Due to their high destruction and removal efficiency (DRE), the thermal processes have been increasingly used for CHCs removal and destruction. Previous studies of the combustion chemistry of CHCs indicate that phosgene occurs under both fuel-rich and fuel-lean conditions [3–6]. The maximum concentrations of phosgene found in the flames of CHCs combustion are shown in the Table 1.

COCl_2 can result in bronchoconstriction, pulmonary edema, and immune suppression [7]. The clinical signs of phosgene exposure are chest discomfort, headache and cough [8]. It also causes a significant decrease in lung volume [9] and an increase of lung weight gain [10]. The clinical presentation and lung morphology observed after inhalation of phosgene are similar to those after oxidant gas exposure and include a clinical latent period, generally 12–24 h, followed by noncardiogenic pulmonary edema and death at some time after a significant concentration \times time product is attained [9, 11]. In addition, the phosgene can also increase lipid peroxidation and pulmonary vascular permeability [12]. It has been estimated that the LC₅₀ of phosgene in goats [14] and in sheep [13] was 10 000 and 13 300 mg min/m³, respectively.

The three major sources of phosgene in air are: (1) direct emission during manufacture, handling and use; (2) thermal decomposition of CHCs; and (3) photon-induced oxidation of CHCs [15, 16]. The first two sources can result in a significant indoor hazard, but their contribution to the ambient air is minimal. The photo-oxidation of chloroethylenes (primarily C_2Cl_4 and C_2HCl_3) seems to be the most probable source of phosgene [15, 16].

Table 1
Phosgene formation in the flame of CHCs combustion

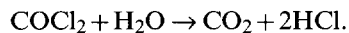
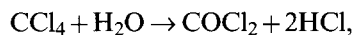
Flame	Equivalence ratio	Cl/H ratio	Maximum COCl_2 concentration (ppm)	References
CCl_4/CH_4	0.80	0.78	3900	[3]
CCl_4/CH_4	1.22	0.64	500	[3]
CCl_4/CH_4	1.92	0.14	760	[3]
CCl_4/CH_4	2.00	0.22	1100	[3]
C_2HCl_3	0.55	3.00	1300	[4]
$\text{CHCl}_3/\text{CH}_4$	2.25	0.24	1500	[5]
$\text{CHCl}_3/\text{CH}_4$	1.75	0.25	2300	[5]
$\text{CHCl}_3/\text{CH}_4$	0.46	1.37	9500	[5]

Phosgene concentrations in the ambient air of more rural and remote locations were found to have no significant seasonal variation and to be approximately at the level of 15–25 ppt [15, 17, 18]. The factor of 1.5 for the phosgene gradient between an urban and a remote site was compared by Singh [15] with a factor of 20 for its precursors (C_2Cl_4 and C_2HCl_3). This difference primarily arises because the precursors come from urban sources and are well dispersed by the time a significant decomposition to phosgene takes place.

Helas and Wilson [16] also proposed that although the decomposition reactions of CHCs for phosgene formation take place everywhere in the troposphere, they have their maximum near the surface. This is due to two reasons: one is the temperature dependence of the OH-initiated phosgene-forming reaction, which is accelerated at the higher temperature prevailing near the surface; the other reason is that the precursor, trichloroethylene, should have a relatively small-scale height, as can be deduced from the large fluctuations of its surface mixing ratios [16, 19].

Methylene chloride is a common ingredient of many paint removers employed by individuals renovating older homes or repairing furniture. It is often used in poorly ventilated areas and may be exposed to a heat source to facilitate paint removal. This condition may result in a risk of phosgene production [8]. There were several previous reports suggesting severe pulmonary injury and death due to phosgene (a combustion product of methylene chloride) poisoning caused by the use of this chemical near a heat source [8]. It is also possible that cigarette smokers may be exposed to an additional dose of phosgene, since chloroethylenes are thermally decomposed to phosgene, and are often present in cigarette smoke at concentration of up to 200 times the ambient phosgene concentration [15].

Gaisinovich and Ketov [20] investigated the kinetics of the vapor-phase hydrolysis of CCl_4 in the range 350–550 °C by using high-temperature infrared spectroscopy, and phosgene was detected in the hydrolysis products. The hydrolysis of $COCl_2$ at 220–420 °C took place according to a second-order equation. Their reaction equations were as follows:



In addition, the rates of hydrolysis of $COCl_2$ were 10 and 35 times of magnitude greater than those of CCl_4 at 450 °C and 350 °C, respectively [20].

1,1-dichloroethylene (DCE) is one of the major industrial chemicals and a common environmental pollutant. A high exposure concentration of DCE can damage the eyes, skin, heart/blood, and nervous system. DCE decomposition by using a radio-frequency (RF) plasma system is an innovative technique. By enforcing a continuous electrical-voltage with a varied frequency, organic-gas molecules like DCE are decomposed into electrons, ions, free radicals, atoms, and other neutral molecules that form the glow discharge. The temperature of the gas molecule in an RF plasma reactor is near room temperature, while the temperature of electron is higher than 2000 °C. At such high temperature, the energy of an electron is approximately 50 kcal/mol, which is twice higher in magnitude than the activation energy

of a conventional chemical reaction (25 kcal/mol). Therefore, the conventional reaction which needs to proceed at a very high temperature will be finished at a lower temperature in the RF plasma reactor.

In this study, an RF plasma reactor was used to decompose the DCE. The effect of plasma operational-parameters for the DCE decomposition, the fraction of total-carbon converted into CO_2 and CO , and the COCl_2 effluent concentration were investigated. In addition, the reaction mechanism of DCE decomposition and COCl_2 formation are discussed.

2. Experimental

In this study, the RF plasma reactor is a cylindrical glass which has a diameter of 4.14 cm and a height of 15 cm (Fig. 1). The inner copper electrode of cylindrical type has a diameter of 2.55 cm and a height of 3 cm. The outer copper electrode has a height of 5.4 cm and is wrapped on the plasma reactor and grounded. A plasma generator and matching network supply 13.56 MHz RF power to the inner

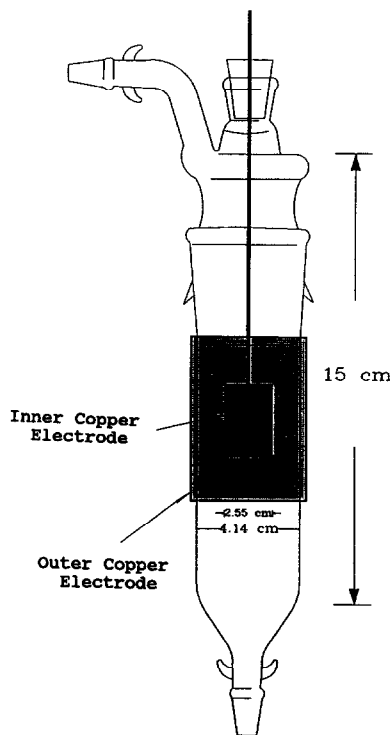


Fig. 1. RF plasma reactor.

copper electrode, which is hollow and serves as a gas-distribution manifold. Gas introduced into the bottom of the reactor flows through glass tubes into the powered electrode where it mixes before flowing into the copper electrode zone. This arrangement ensures that all gas introduced into the reactor flows through the glow discharge.

A mass flow meter was used for the control of feeding gases. The reactor was evacuated through the center of the reactor at low pressure (1–5 torr). This arrangement ensured radially symmetric flow profiles which helped in minimizing radial concentration gradients between the glow discharge and the glass walls. The gaseous product species out of the reactor is on-line introduced into a Fourier transform infrared (FTIR) spectrometer (Bio-Rad, Model FTS-7) for the species identification and quantification (Fig. 2). Before the experiment, a diffusion pump was used to keep the system pressure lower than 0.001 torr for the clean-up of contamination. Calibration of gaseous reactants and product species was made by withdrawing unreacted standard gases and by directly going through the sampling line connected to the FTIR. The mass of the species was calculated by comparing the response factor (absorbance height/concentration) of standard gas at the same IR wave number. The wave numbers of both absorbance-zone range and -peak center for 11 species are shown in Table 2. All of these 11 species were identified and quantified in this study. Due to the deposition and condensation occurring in the sampling and analyzing system, the FTIR quantification data for H₂O and HCl were unreliable. The concentrations of H₂O and HCl were determined through O-atom and Cl-atom balances, respectively.

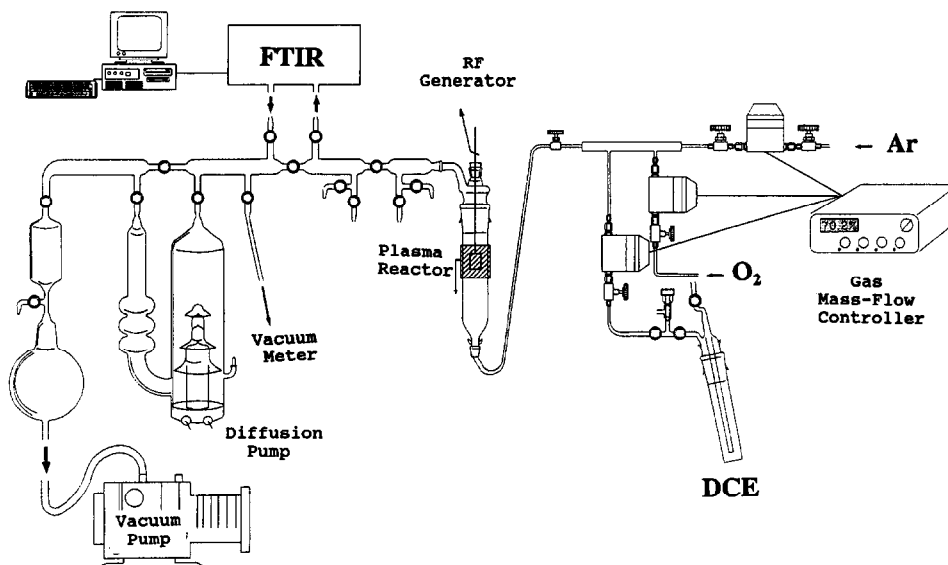


Fig. 2. The feeding and sampling system.

Table 2
The FTIR Wavenumbers of absorbance-zone range and -peak center for 11 species

Species	The wave numbers of absorbance-zone range (cm ⁻¹)	The wave numbers of absorbance-peak center (cm ⁻¹)
1,1-C ₂ H ₂ Cl ₂	418–497	457
	556–652	597, 609
	825–955	793, 801, 867
	1040–1170	1131, 1146, 1085
	1510–1660	1562, 1576, 1627
CO ₂	655–680	667
	2230–2400	2355, 2332
CO	1970–2230	2176, 2112
COCl ₂	1710–1890	1830
C ₂ H ₂	640–840	729, 764
	1250–1445	1297, 1348
	3170–3400	3255, 3305
H ₂ O	2900–4200	3710
	1200–2200	1590
	500–1000	500
C ₂ HCl ₃	816–878	849
	878–963	935, 944
C ₂ Cl ₄	737–822	782, 801
	879–938	916
CHCl ₃	721–782	771
	1192–1245	1218
CCL ₄	724–834	774, 795
C ₂ H ₂ Cl ₂ O	680–825	718, 785
	870–1100	964, 991, 1048
	1730–1870	1799, 1828

3. Results and discussion

In the plasma reactor, the DCE decomposition fraction was primarily affected by the DCE concentration in the feeding gas mixtures, the equivalence ratio (ϕ = stoichiometric O₂ needed/actual O₂ used) of feeding gas mixtures, the input power wattage and the gas flow rate in the reactor. In this study, the focus of the results and discussion is on the DCE decomposition fraction, the COCl₂ effluent concentration, the carbon balance and the fraction of total carbon input converted into CO₂ and CO. The data associated with other species shown in Table 2 will be published elsewhere.

3.1. Steady state of the reaction

In this study, each run of experiment lasted for 30 min and the effluent concentration of individual species was monitored by the FTIR from the start of reaction to 25 min. Steady state was easily reached for the conditions of lower DCE feeding concentrations. In general, the steady state was reached after 20 min for all

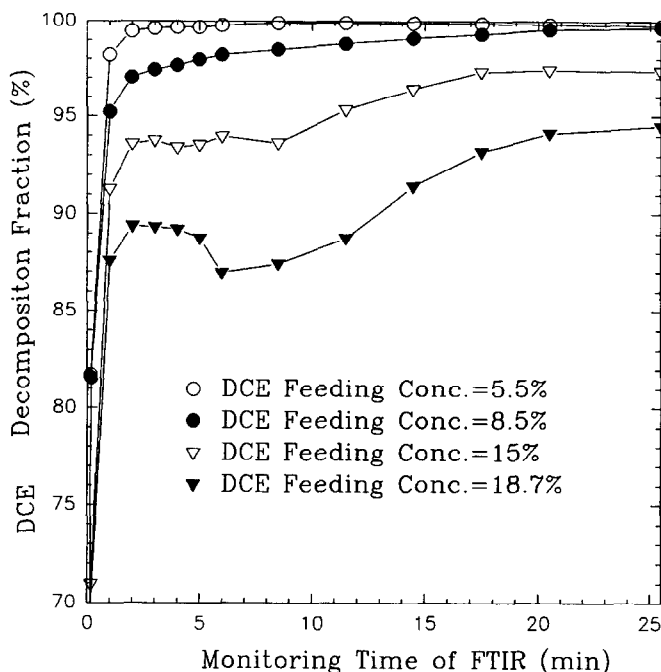


Fig. 3. The DCE decomposition fraction versus monitoring time of FTIR.

experiments (Fig. 3). Therefore, the effluent concentration of each species was calculated by using the mean value of measured data after 20 min.

3.2. Effect of DCE concentration in the feeding gas mixtures

In this investigation, argon was used as the carrier gas; equivalence ratio (ϕ) was controlled at 1.0; operational pressure was 3.4 torr; power wattage was 20 W; gas total-flow rate was 14.8 sccm; and the DCE concentrations in the feeding gas mixtures were varied between 5.5% and 18.7% (Figs. 4 and 5).

As the equivalence ratio remained constant ($\phi = 1.0$), the decreasing of the DCE concentration increased the relative concentration of argon. In the plasma reactor, argon used for the carrier gas also acted as the energy transfer medium. The higher concentration of argon in the feeding gas mixtures results in a higher concentration of excited Ar^* in the plasma reactor and therefore in an increased DCE collision frequency and an elevation of the DCE decomposition efficiency. Fig. 4 shows that when feeding DCE concentrations were increased from 5.5% to 18.7%, the DCE decomposition fraction was decreased from 99.9% to 93.2%.

However, the absolute molecules of reacted DCE are calculated as $5.5\% \times 99.9\%$ at feed DCE concentration of 5.5% and $18.7\% \times 93.2\%$ at the DCE of 18.7%, which leads to the ratio 549:1743. This means that the reaction probabilities at higher concentrations of DCE, e.g. 18.7%, are far larger than those at the lower feed, e.g. 5.5%.

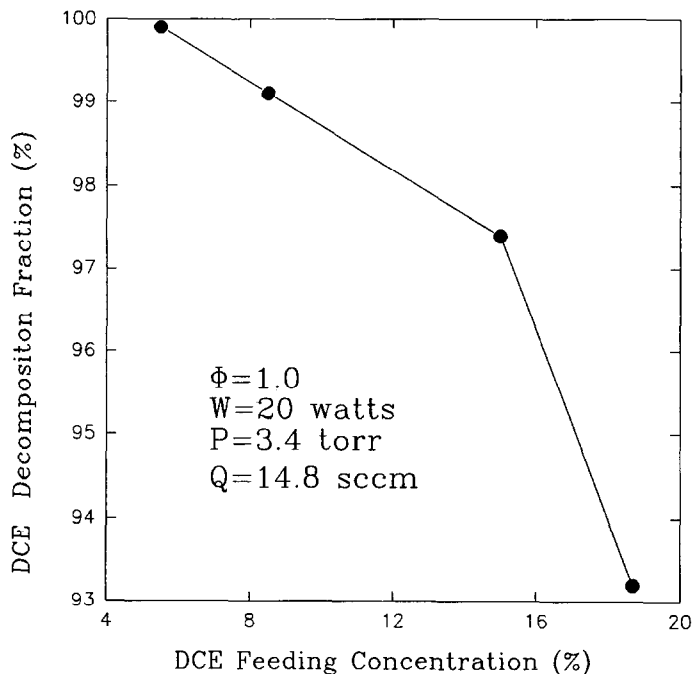


Fig. 4. The correlation between DCE feeding concentration and its decomposition fraction.

The destruction and removal efficiency (DRE) of chlorinated hydrocarbons (CHCs) expressed only by the reactant disappearance fraction was not satisfied for practical applications. The additional parameter was the $[\text{CO}_2 + \text{CO}]$ conversion fraction (%), which was defined as the fraction (%) of total carbon input converted into CO_2 and CO . Fig. 5 shows that when DCE feeding concentrations were increased from 5.5% to 18.7%, the fraction of total carbon $[\text{CO}_2 + \text{CO}]$ decreased from 42.9% to 17.3%. These results indicate that large admission of DCE reduced the possibility of CO_2 and CO formation. In addition, increasing the DCE feeding concentration may decrease the concentration of excited Ar^* in the plasma reactor, weaken the plasma state and, therefore, make the reaction more incomplete.

The COCl_2 effluent concentration was increased by increasing the DCE feeding concentration. This findings are explained in terms of a higher possibility for COCl_2 formation due to the more abundant C and Cl sources arising from higher feeding of DCE. The carbon balance is defined as the total carbon mass in the effluent gas stream divided by the total carbon mass in the feeding gas stream. The carbon in the soot is not included for the carbon-balance calculation. Although the data of C_2H_2 , C_2HCl_3 , C_2Cl_4 , CHCl_3 , CCl_4 and $\text{C}_2\text{H}_2\text{Cl}_2\text{O}$ were not presented in this paper, these species were also calculated and included for the carbon balance. Fig. 5 showed carbon balance ranged between 0.89 and 1.01 and averaged 0.95. These results revealed that carbon loss from the soot formation was not significant in these operational conditions.

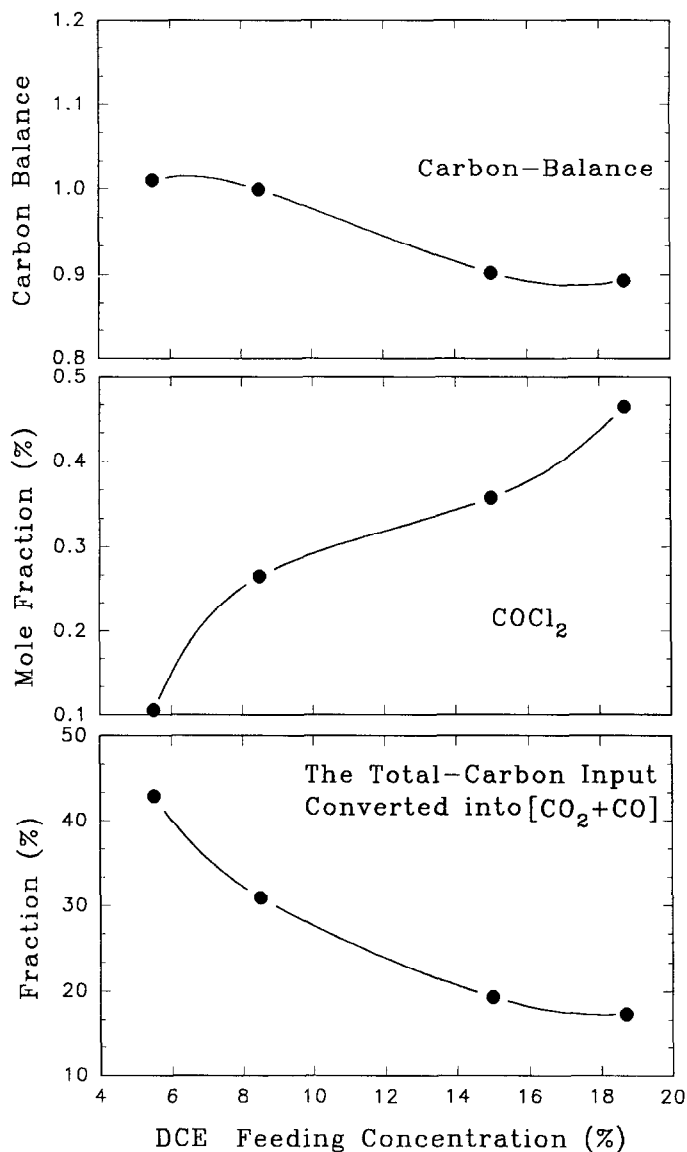


Fig. 5. The effect of DCE feeding concentration for carbon balance, COCl₂ effluent concentration, and the fraction of total-carbon converted into CO₂ and CO.

3.3. Effect of the equivalence ratios

In this investigation, operational pressure was controlled at 3.4 torr; the flow rate was 14.8 sccm; the input power wattage was 20 W. Argon was used as a carrier gas. The equivalence ratio ϕ varied as 0.69, 0.82, 1.0, 1.8 and 3.0. When ϕ was at a range between 0.69 and 1.8, a higher ϕ value was found to have a higher

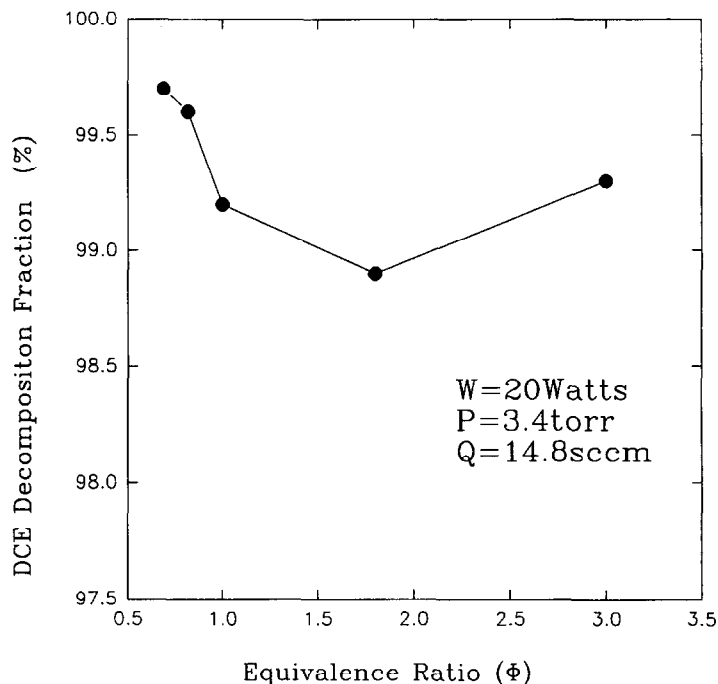


Fig. 6. The effect of equivalence ratio for DCE decomposition fraction.

DCE decomposition fraction (Fig. 6). This indicated that higher ϕ value provided less oxygen in the reactor and reduced the possibility of DCE oxidation. However, when ϕ increased from 1.8 to 3.0, the concentration of oxygen was lower and the oxidation effect of DCE was minor. The concentration ratio of Ar/O₂ was increased very significantly. At the same input power wattage, the energy transfer efficiency of Ar plasma was higher than that of O₂. This condition resulted in the increasing of effective collision frequency among the reactants, excited Ar (Ar*) and free electron (e⁻), and in elevating the DCE decomposition efficiency.

At higher ϕ values, more soot formation was found in the plasma reactor. This resulted in a lower carbon balance in the effluent gas stream (Fig. 7). The carbon fraction converted into [CO₂ + CO] was decreased very significantly at a ϕ value between 0.82 and 1.8. Less oxygen feeding concentration hindered DCE oxidation and reduced the possibility of both CO₂ and CO formation. Except the atom C and Cl, the formation of more COCl₂ needs more oxygen supply. At a higher equivalence ratio ϕ , the feeding concentration of oxygen was lower and resulted in less COCl₂ formation (Fig. 7).

3.4. Effect of input power wattage

In this investigation, the gas flow rate was 14.8 sccm; the DCE concentration in the feeding gas mixtures was controlled at 8.5%; the equivalence ratio was 1.0;

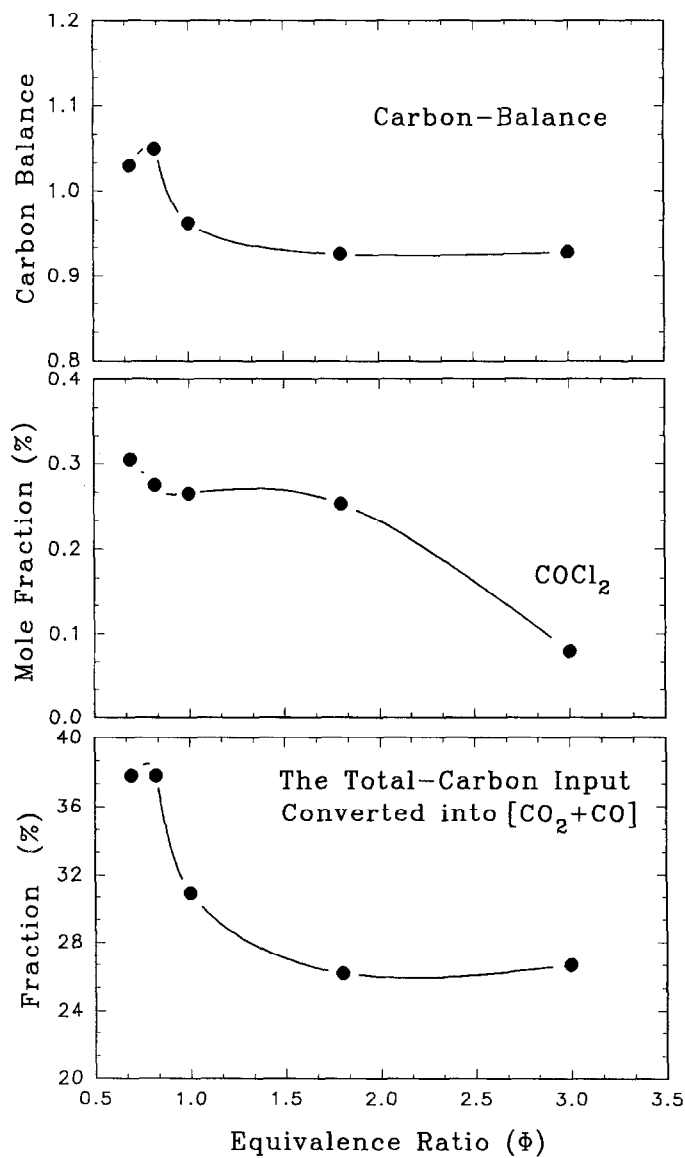


Fig. 7. The effect of equivalence ratio for carbon balance, COCl₂ effluent concentration, and the fraction of total-carbon converted into CO₂ and CO.

the operational pressure was 3.4 torr; and Ar was introduced as the carrier gas. Fig. 8 showed that the DCE decomposition fraction was higher at 60 and 80 W. Higher input power wattage provided more energy for the ionization of gas molecules, increased the effective collision frequency among the reactants, excited

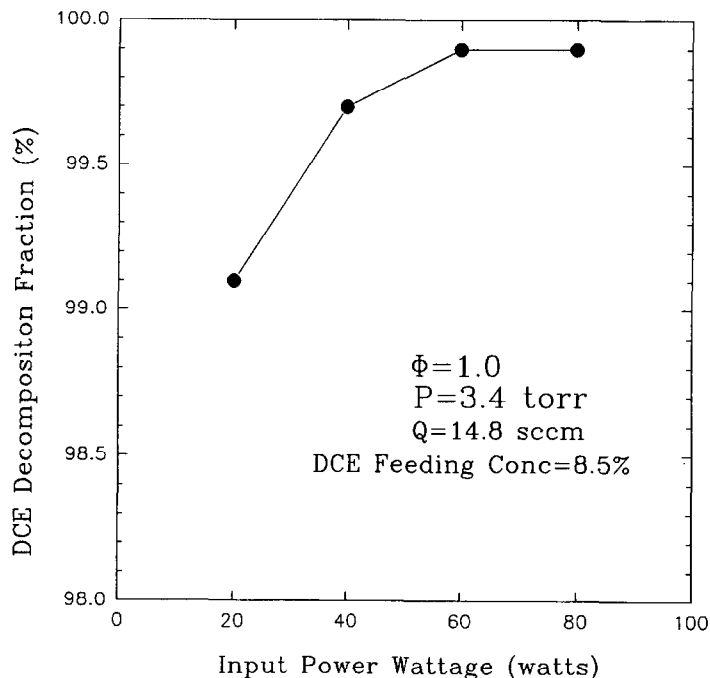


Fig. 8. The effect of input power wattage for DCE decomposition fraction.

the Ar (Ar^*) and free electron (e^-), and therefore, elevated both the DCE decomposition fractions and the total carbon fraction converted into CO_2 and CO. Due to the fact that more DCE was converted into CO and CO_2 and the reaction pathway for COCl_2 formation was hindered, the effluent COCl_2 concentration was decreased by increasing the input power wattage. However, more soot formation occurred in the plasma reactor, resulting in a lower carbon balance in the effluent gas stream (Fig. 9).

3.5. Effect of gas flow rate

A lower gas flow rate will increase the gas residence-time in the reactor and make the reaction proceed more completely. Fig. 10 shows that the DCE decomposition fraction is decreased by increasing the gas flow rate in the reactor. Particularly, when the gas flow rate was between 10.8 and 14.8 sccm, the DCE decomposition fraction decreased very rapidly. The total carbon fraction converted into CO_2 and CO was also decreased by increasing the gas flow rate (Fig. 11). However, no significant trends were found for the COCl_2 concentration and carbon balance.

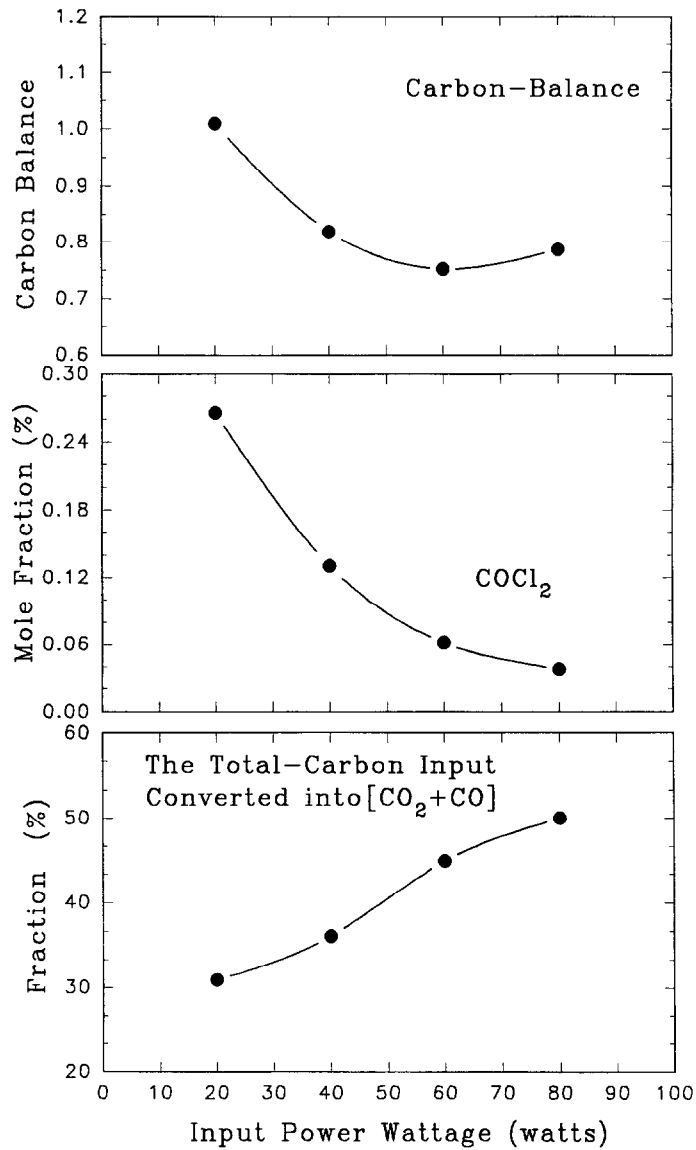


Fig. 9. The effect of input power wattage for carbon balance, COCl₂ effluent concentration, and the fraction of total-carbon converted into CO₂ and CO.

3.6. Possible reaction pathway for the DCE decomposition

The DEC decomposition was mostly by self-dissociation or by attack by the e⁻, O, Cl, or OH. The reaction mechanism was as follows:

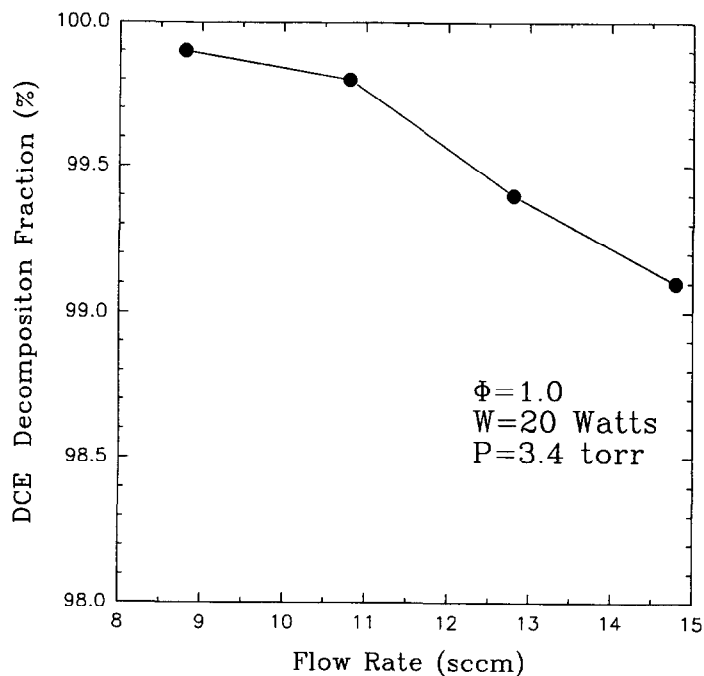
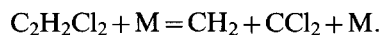
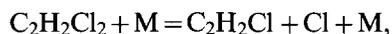
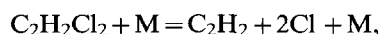
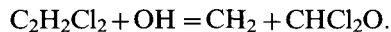
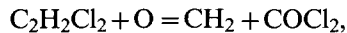
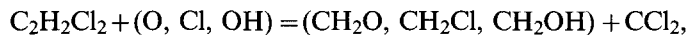
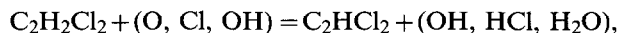


Fig. 10. The effect of gas flow rate for DCE decomposition fraction.

1. self-dissociation in the inert bath



2. Attacked by the e^- , O, Cl, or OH



3.7. COCl_2 formation mechanism

C_2Cl_4 , CHCl_3 and CCl_4 were detected in the effluent gas stream. These products may act as intermediate species to form COCl_2 . The C_2Cl_4 or C_2Cl_3 may be attacked by the OH and O_2 , respectively.

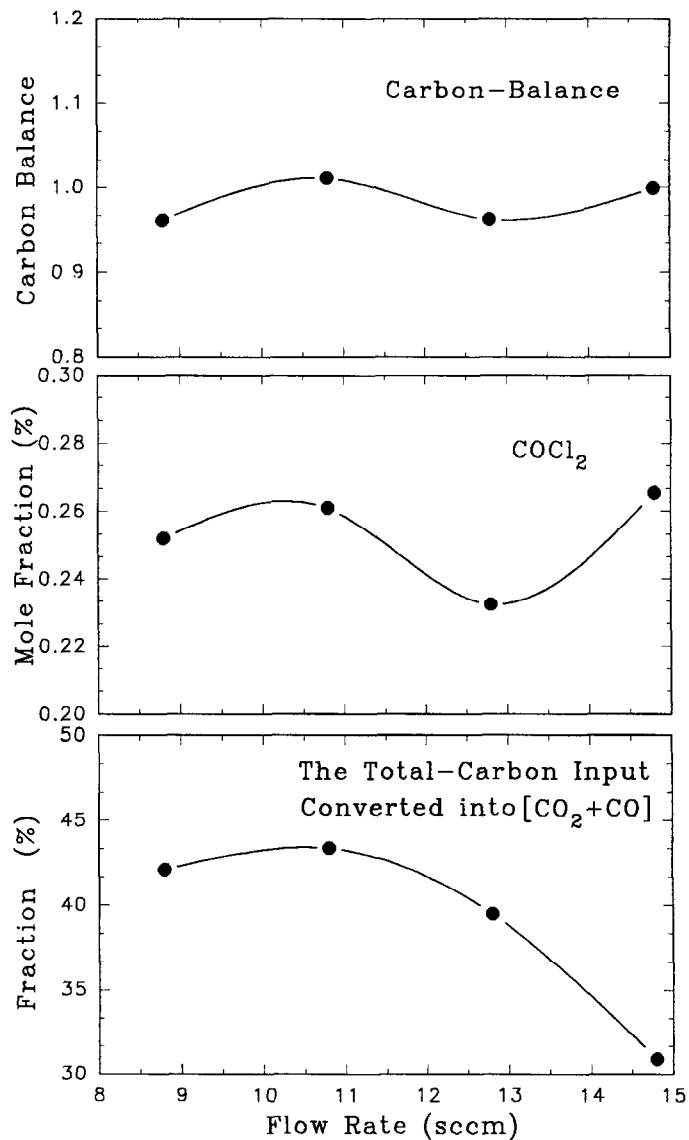
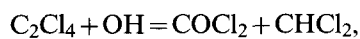
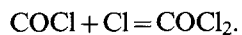


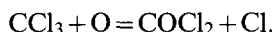
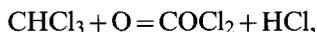
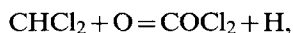
Fig. 11. The effect of gas flow rate for carbon balance, COCl_2 effluent concentration, and the fraction of total-carbon converted into CO_2 and CO .



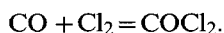
COCl_2 was probably formed from the combination of COCl with Cl .



The COCl_2 may also form from the CHCl_2 , CHCl_3 and CCl_3 which was attacked by the O or O_2 , respectively.

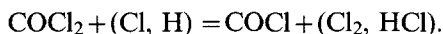


In addition, copper used for copper electrode in the plasma reactor seems to act as a catalyst for the activation to form atomic chlorine. The catalytic reaction of CO and Cl_2 on Cu catalyst is

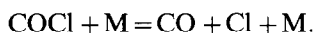


3.8. Decomposition of COCl_2

COCl_2 was easily attacked by both Cl and H radicals and decomposed.



COCl can be further decomposed into CO and Cl.



In addition, COCl_2 can also be decomposed directly into CO and Cl_2 .



4. Conclusions

1. In this plasma reactor, the steady state was reached before 20 min for all experiments.
2. Both DCE decomposition efficiency and the fraction of total carbon mass converted into CO_2 and CO were decreased by increasing the DCE feeding concentration.
3. The DCE decomposition efficiency at varied equivalence ratios (ϕ) was controlled by both oxidation and energy transfer efficiency.
4. At lower equivalence ratios, a greater amount of COCl_2 was formed due to the higher oxygen feeding concentration.
5. Higher input power wattage can increase both DCE decomposition efficiency and the fraction of total-carbon mass converted into CO_2 and CO and reduce the COCl_2 effluent concentration. However, more soot was found in the plasma reactor when the input power wattage was higher than 60 W.
6. The possible reaction pathways for DCE decomposition are self-dissociation or attack by the e^- , O, Cl and OH.
7. Because high concentrations of C_2Cl_4 , CHCl_3 and CCl_4 were detected, in the plasma reactor, the possible reaction pathways for the COCl_2 formation were $\text{C}_2\text{Cl}_4 + \text{OH}$, $\text{C}_2\text{Cl}_3 + \text{O}_2$, $\text{CHCl}_3 + \text{O}$, $\text{CHCl}_2 + \text{O}$, $\text{CCl}_3 + \text{O}$ and $\text{CO} + \text{Cl}_2$.

Acknowledgements

This research was supported, in part, by the National Science Council, Taiwan, grant No. NSC-83-0410-E-006-057.

References

- [1] D. Grosjean, *J. Air. Waste Manage. Assoc.*, 41 (1991) 56.
- [2] G.K. Rollefson and C.C. Montgomery, *J. Am. Chem. Soc.*, 5 (1933) 142.
- [3] M. Xieqi, B. Cicek, S. M. Senkan, *Combust. Flame*, 94 (1993) 131.
- [4] W.D. Chang, S.B. Karra and S.M. Senkan, *Environ. Sci. Technol.*, 20 (1986) 1243.
- [5] W.J. Lee, B. Cicek and S.M. Senkan, *Environ. Sci. Technol.*, 3 (1993) 949.
- [6] W.D. Chang, S.B. Karra and S.M. Senkan, *Combust. Sci. Technol.*, 49 (1986) 107.
- [7] M.C. Madden, M. Friedman, L.L. Keyes, H.S. Koren and G.R. Burleson, *Inhal. Toxic.*, 3 (1991) 3.
- [8] R.W. Synder, H.S. Mishel and G.C. Christensen, *Chest*, 101 (1992) 860.
- [9] A.J. Ghio, T.P. Kennedy, G.E. Hatch and J.S. Tepper, *J. Appl. Physiol.*, 71 (1991) 657.
- [10] Y.L. Guo, T.P. Kennedy, J.R. Michael, A.M. Sciuto, A.J. Ghio, N.F. Adkinson JR. and G.H. Gurtner, *J. Appl. Physiol.*, 69 (1990) 1615.
- [11] W.F. Diller, *Toxicol. Ind. Health*, 1 (1985) 7.
- [12] T.P. Kennedy, J.R. Michael, J.R. Hoidal, D. Hasty, A.M. Sciuto, C. Hopkins, R. Lazar, G.K. Bysani, E. Tolley and G.H. Gurtner, *J. Appl. Physiol.*, 67 (1989) 2542.
- [13] J.R. Keeler, H.H. Hurt, J.B. Nold and W.J. Lennox, *Drug Chem. Toxic.*, 13 (1990) 229.
- [14] W.F. Diller and R. Zante, *Zbl. Arbeitsmed*, 32 (1982) 360.
- [15] H.B. Singh, *Nature*, 264 (1976) 428.
- [16] G. Helas and S.R. Wilson, *Atmos. Environ.*, 26A (1992) 2975.
- [17] H.B. Singh, L.J. Salas, A.J. Smith and H. Shigeishi, *Atmos. Environ.*, 15 (1981) 601.
- [18] S.R. Wilson, P.J. Crutzen, G. Schuster, D.W.T. Griffith and G. Helas, *Nature*, 334 (1988) 689.
- [19] H.B. Singh, L. Salas, H. Shigeishi and A. Crawford, *Atmos. Environ.*, 11 (1977) 819.
- [20] M.S. Gaisinovich and A.N. Ketov, *Russ. J. Inorg. Chem.*, 14 (1969) 1218.